Available online at www.sciencedirect.com

SCIENCE DIRECT

ELSEVIER

Genomics 87 (2006) 463–473

GENOMICS

www.elsevier.com/locate/ygeno

Transcription of human neuronal nitric oxide synthase mRNAs derived from different first exons is partly controlled by exon 1-specific promoter sequences

Matthias Bros [a], Jean-Paul Boissel [b], Ute Gödtel-Armbrust [b], Ulrich Förstermann [b,*]

[a] *Department of Dermatology, Johannes Gutenberg University, D-55101 Mainz, Germany*
[b] *Department of Pharmacology, Johannes Gutenberg University, D-55101 Mainz, Germany*

Received 7 July 2005; accepted 24 November 2005
Available online 18 January 2006

Abstract

The human neuronal nitric oxide synthase (*NOS1*) gene is subject to extensive splicing. A total of 12 *NOS1* mRNA species have been identified. They differ in their 5′ ends and are derived from 12 different first exons (termed exons 1a to 1l). Various cell lines whose *NOS1* first exon expression patterns were representative of human brain, skin, and skeletal muscle were identified. These included A673 neuroepithelioma cells, SK-N-MC neuroblastoma cells, HaCaT keratinocyte-like cells, and C2C12 myocyte-like cells. In these cell lines, correlations were found between the exon 1 variants preferentially expressed and the promoter activities of their cognate 5′ flanking sequences. These data demonstrate that expression of the different exon 1-related splice variants of *NOS1* mRNA is controlled directly (at least in part) by the associated 5′ flanking sequences.

Keywords: Alternative splicing; Reporter gene assays; RT real-time PCR; Cortex; Hippocampus; Skin; Skeletal muscle; Heart; Testis; Kidney

Both neuronal and nonneuronal cells and tissues are known to express neuronal-type nitric oxide synthase (*NOS1*) [1]. In brain, nitric oxide (NO) produced by *NOS1* is known to function as a modulator of neuronal function affecting the release of neurotransmitters and playing a role in long-term potentiation as well as in long-term depression [2]. In peripheral tissues, numerous other functions have been attributed to *NOS1*, such as modification of skeletal muscle contractile force or control of total body Na^+ [3]. In addition, various conditions have been described in which concentrations of NO rapidly increase (e.g., ischemia–reperfusion injury or glutamate-mediated neurodegenerative processes in the CNS). The molecular mechanisms involved in these disorders include both hyperactivation of the *NOS1* enzyme and upregulated expression of the *NOS1* gene [4]. Structural mRNA diversity is a hallmark of *NOS1* expression and expressional regulation seems unusually complex [5,6]. In addition to cell-specific *NOS1* mRNA splicing, we have previously found stimulus-dependent switches in the predominant *NOS1* mRNA expressed in a given cell [7].

Given the relevance of *NOS1* in both physiology and pathophysiology, and the important consequences of altered expression, a profound understanding of the regulatory network appears to be critical. Therefore, the current study was undertaken to investigate the mechanisms controlling the expression of the various *NOS1* splice forms in different cell types. We generated numerous reporter gene constructs to test the potential function of exon 1-associated 5′ flanking sequences for the transcription of the different *NOS1* splice variants.

Results

Cell-type-specific expression of human NOS1 exon 1 variants

We have recently demonstrated transcriptional usage of 10 different *NOS1* exon 1 variants, expressed in a cell-type- and

* Corresponding author. Fax: +49 6131 393 6588.
E-mail address: ulrich.forstermann@uni-mainz.de (U. Förstermann).

0888-7543/$ - see front matter © 2005 Elsevier Inc. All rights reserved.
doi:10.1016/j.ygeno.2005.11.013

stimulus-dependent manner in various human tissues [6]. In this study, we have applied reverse transcriptase (RT) real-time PCR analysis to quantify the relative expression levels of the various exon 1 variants in human tissues.

As depicted in Fig. 1, human cerebral cortex and hippocampus showed comparable expression patterns characterized by a predominant usage of exons 1d, 1f, and 1g. In cerebral cortex, *NOS1* messages containing one of these exons were expressed at comparable transcriptional levels (20–30%), in hippocampus about half of all *NOS1* transcripts contained exon 1d. In both brain regions, exon 1k-containing *NOS1* mRNA was significantly less abundant (below 10%). In cerebral cortex, we also found a low level of expression of exons 1b and 1l ("one ell") (6 and 11%, respectively). In skin, other exon 1 variants were expressed at significant levels: exons 1d (40%), 1b (25%), and 1f (18%) accounted for the majority of the *NOS1* transcripts, minor transcripts contained exon 1g (10%) and exon 1j (7%) (Fig. 1). In heart, the dominant *NOS1* transcripts contained either exon 1d or exon 1g (29 and 39%, respectively). In addition, exon 1k was detected in about 15% of the *NOS1* mRNA. Exons 1b, 1f, and 1l were expressed at lower levels, each accounting for less than 10% of the total. In contrast, in

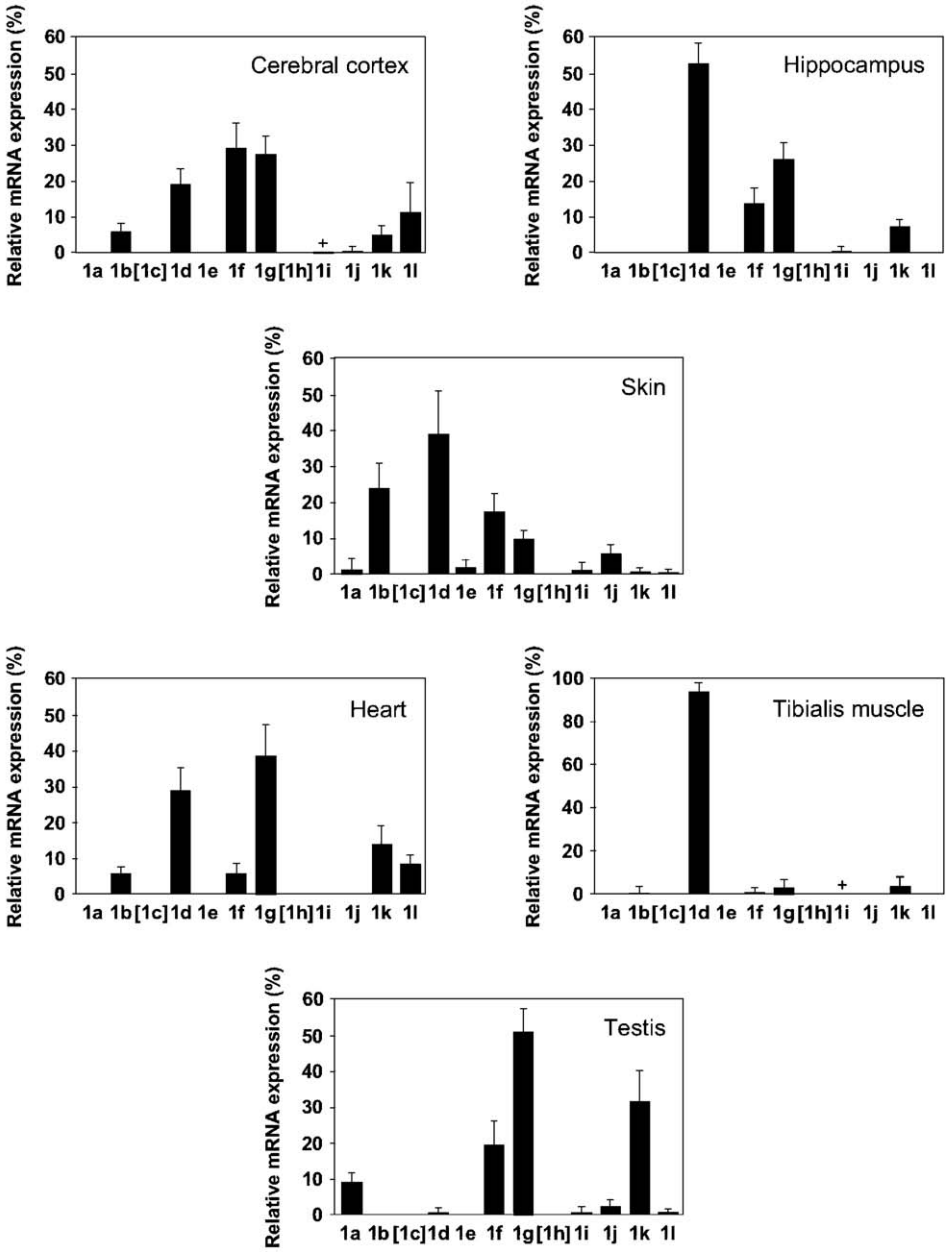

Fig. 1. Expression of *NOS1* mRNA splice variants in biopsies of human tissues. Transcriptional diversity of *NOS1* mRNA expression (the use of different first exons) was assessed using RT real-time PCR. Sequences of the first exon-specific sense primers (to exons 1a to 1l), of the common exon 2-specific antisense primer, and of the exon 2-specific TaqMan probe are indicated in Table 1 and under Materials and Methods. The following human tissues were analyzed: cerebral cortex, hippocampus, tibialis muscle, heart, ileum, skin, kidney, testis. Two additional first exons (1c) and (1h) reported by Wang et al. [5], but not detected by us in a previous study [6], are indicated, but were not investigated because classical PCR failed to amplify specific 1c and 1h fragments (not shown). Data represent means ± SEM of three independent RNA preparations; +, transcripts detected, but representing less than 0.2% of the total *NOS1* mRNA.

tibialis muscle, *NOS1* message contained almost exclusively exon 1d. All other transcripts accounted for less than 5% of the total *NOS1* mRNA (Fig. 1). In testis, the majority of *NOS1* transcripts contained exon 1g (50%), exon 1k (33%), or exon 1f (21%). Exon 1a accounted for about 9% of total *NOS1* mRNA (Fig. 1). In ileum, *NOS1* mRNA contained predominantly exon 1f (50%) or exon 1d (35%); exons 1g and 1k accounted for less than 10% of total *NOS1* mRNA (data not shown). In kidney, quantitative PCR confirmed our previous finding of almost exclusive usage of exon 1d (96%). Trace amounts of *NOS1* transcripts harboring exons 1f, 1g, and 1k were also found (data not shown).

Thus, in many cases exons 1d, 1f, and 1g were expressed in parallel and accounted for the majority of *NOS1* transcripts. Exon 1k was expressed in all tissues analyzed, albeit at varying levels. We have shown recently that exon 1k is often spliced in between another exon 1 located more upstream in the *NOS1* gene and the common exon 2 [6]. Also in the current study, we found exon 1k inserted between exon 1g and exon 2 in cerebral cortex (20% of exon 1g-containing *NOS1* mRNA) and in skin (65% of exon 1g-containing *NOS1* mRNA, data not shown).

Promoter test constructs for the multiple NOS1 exon 1 variants

To examine whether the transcription of the numerous *NOS1* exon 1 variants was regulated by promoter activity of the respective upstream flanking genomic regions, we used overlapping PAC clones spanning the genomic region of the human *NOS1* gene (Fig. 2A) to generate corresponding promoter reporter constructs for each exon 1 variant. As depicted in Fig. 2B, these reporter constructs covered several kilobases of genomic sequence for most exons to ensure that all relevant *cis*-acting elements were covered. An additional set of truncated reporter constructs spanning the putative core promoter regions was also generated to exclude the possibility of promoter interference (Fig. 2B).

NOS1 exon 1 expression pattern in NOS1-expressing cell lines

Given the importance of *NOS1*-derived NO for brain function and its role in neurodegenerative diseases, we tested the *NOS1* promoter constructs in the neuroepithelioma cell line A673 and the neuroblastoma cell line SK-N-MC (Fig. 3). Both cell types express significant levels of *NOS1* [6,7]. Due to the relevance of *NOS1* for skin proliferation and wound healing, we included the *NOS1*-expressing keratinocytic cell line HaCaT in our studies [8] (Fig. 3). Considering the role of *NOS1* in skeletal muscle function and its potential involvement in muscular dystrophy, we aimed at testing the *NOS1* promoter constructs in a respective cell line. However, there is no *NOS1*-expressing human skeletal muscle cell line. Therefore, these experiments were performed in the *NOS1*-expressing murine myoblast cell line C2C12 [9] (Fig. 3).

Quantitative PCR analyses revealed a similar *NOS1* exon 1 expression pattern in A673 cells and SK-N-MC cells characterized by a predominant usage of exons 1f, 1g, and 1k (Fig. 3, left). Whereas in A673 cells exon 1g accounted for 50% of *NOS1* transcripts and the adjacent exon 1f for an additional 29% of *NOS1* mRNA, the ratio was reversed in SK-N-MC cells. Here exon 1f was present in 51% of *NOS1* transcripts and exon 1g found in 20% of the *NOS1* mRNA (Fig. 3, left). Exon 1k was expressed at the same level in either cell line (about 20% of all *NOS1* transcripts, Fig. 3, left). Thus, with the exception of underrepresented exon 1d, the overall *NOS1* expression patterns in A673- and SK-N-MC cells were similar to those observed in brain tissue (see Fig. 1).

In the human keratinocytic cell line HaCaT, exon 1g-containing *NOS1* transcripts were the dominant mRNA species (59%); exons 1f and 1i were expressed at somewhat lower levels (around 25% each), followed by exon 1k (about 15%). So far, the expression pattern is similar to the *NOS1* exon 1 pattern found in skin (see Fig. 1). However, exons 1b and 1d, which contributed to *NOS1* expression in skin (Fig. 1), were not found expressed in HaCaT cells.

Promoter function of NOS1 exon 1 5′ flanking genomic regions in representative cell lines

As suggested by the high abundance of exon 1g-containing *NOS1* transcripts in A673 cells (Fig. 3, left), the exon 1g full-length promoter test construct was 7.5-fold as active as the promoterless pGL3-Basic vector. Interestingly, the activity of the core promoter region of exon 1g was even 32-fold that of pGL3-Basic (Fig. 3, right). Despite the high expression of exon 1f in A673 cells, the corresponding full-length promoter showed only 2-fold activity over pGL3-Basic, the truncated construct was four times more active than pGL3-Basic. This suggests that the expression of exons 1f and 1g may be negatively regulated by more distant *cis*-acting elements. In accordance with the significant expression of exon 1k-containing *NOS1* transcripts in A673 cells, the full-length promoter of exon 1k showed significant activity (14-fold that of pGL3-Basic). The marginal activity of the corresponding deletion construct indicated that expression of exon 1k relied essentially on *cis*-acting elements located upstream of the exon 1j sequence region (which were deleted in the truncated construct, see Fig. 2B). Corresponding to the low expression levels of exons 1b, 1c, 1d 1e, 1i, 1j, and 1l in A673 cells (Fig. 3, left), the respective reporter gene constructs displayed low-to-moderate activity compared with pGL3-Basic (Fig. 3, right).

Surprisingly, the full-length promoter construct for exon 1a, which was barely expressed in A673 cells, showed substantial promoter activity (17-fold over pGL3-Basic). The even greater reporter gene activity (138-fold over pGL3-Basic) for the respective truncated core promoter construct suggests that transcriptional expression of exon 1a is negatively regulated by a *cis*-acting region located in the 5′ part of the promoter region. It is not clear why the exon 1a-related promoter activity does not result in expression of exon 1a in A673 cells (Fig. 3, left). It is possible that the repressive potential of the 5′ part of the promoter region may be stronger in intact cells than detected by transient promoter analysis.

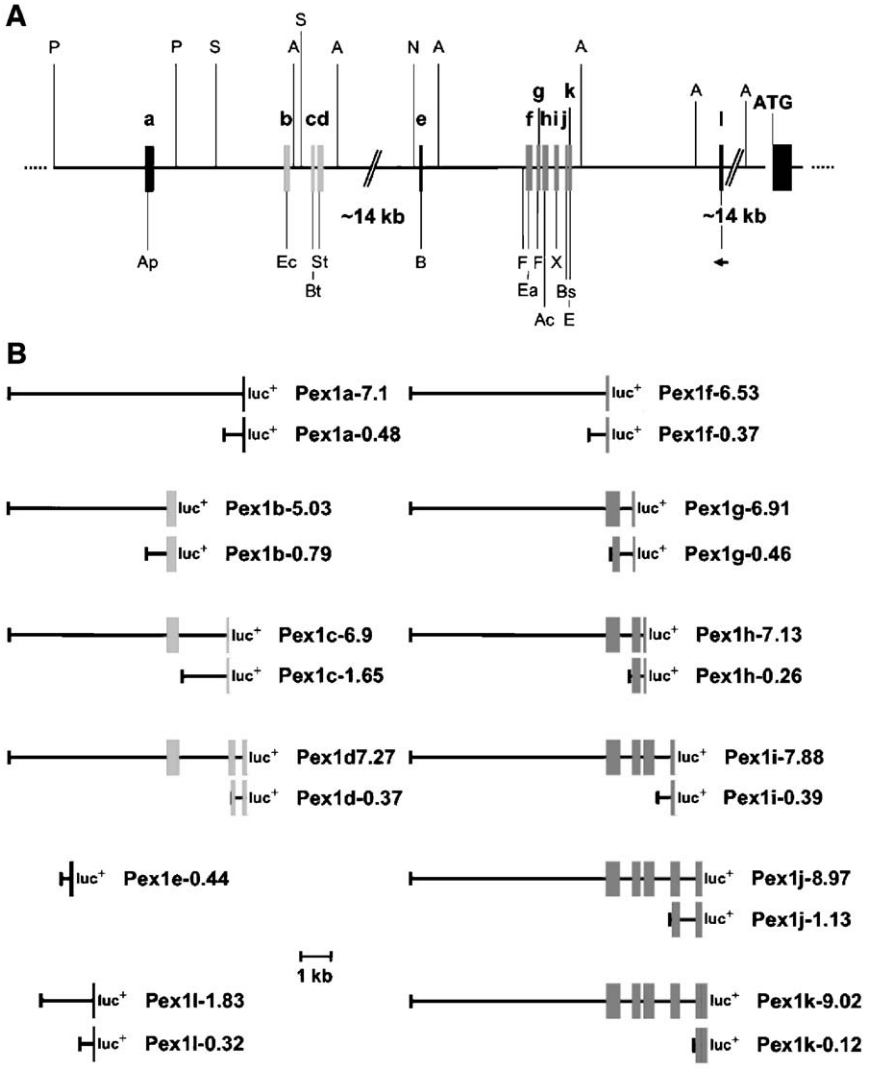

Fig. 2. Organization of the 5′ end of the human *NOS1* gene and schematic representation of the putative promoter-luciferase test constructs pertaining to the different first exons of *NOS1*. (A) Schematic representation of the 5′ end of the human *NOS1* gene showing the localization of the 12 distinct first exons (1a to 1l) and of exon 2 (boxes). The position of the translation start codon (ATG) on exon 2 is indicated. Relevant restriction sites used during the initial cloning steps (cloning of PAC clone fragments into plasmid pZero-2.1) are indicated above the horizontal line representing the genomic DNA sequence. Restriction sites used for subcloning of putative promoter sequences into the *Photinus* luciferase-containing vector pGL3-Basic are shown below the horizontal line. A, *Acc*65I; Ac, *Acc*I; Ap, *Apa*LI; B, *Bam*HI; Bs, *Bsa*I; Bt, *Bst*API; E, *Eco*RI; Ea, *Eag*I; Ec, *Ecl*136II; F, *Fsp*I; N, *Nhe*I; P, *Pst*I; S, *Sma*I; Sc, *Sca*I; St, *Stu*I; X, *Xba*I. The arrow under exon 1l indicates the specific antisense primer used for the cloning of the corresponding promoter construct. (B) Scheme of the 5′ flanking regions of the different first exons of human *NOS1* (exons 1a to 1l) and 5′–3′-deletion constructs thereof (*NOS1* minimal promoter constructs). Proximal 5′ sequences of each first exon 1 were further subcloned in front of the luciferase expression cassette (luc$^+$). Construct names refer to the respective exon 1 sequence and to the length of the remaining 5′ flanking genomic sequence (in kb).

In broad accordance with the endogenous *NOS1* exon 1 expression pattern in the neuroblastoma cell line SK-N-MC cells (Fig. 3, left), the full-length promoter constructs belonging to exons 1f and 1g displayed the highest activity (9.5- and 8-fold over pGL3-Basic, respectively). In contrast to A673 cells, the truncated promoter region of exon 1f exerted reporter activity similar to that of the full-length sequence, whereas the 5′ flanking region of exon 1g showed reduced activity relative to

Fig. 3. Comparison of the expression of the different exon 1-derived splice forms of *NOS1* mRNA in human cell lines with the activities of the *NOS1* promoter reporter gene constructs (Fig. 2B) transfected into the same cells. Left: Quantitative analyses of *NOS1* mRNA splice variants in human A673 neuroepithelioma cells, human SK-N-MC neuroblastoma cells, and human keratinocyte-like HaCaT cells. RT real-time PCR of the different first exon-derived mRNAs was performed as for Fig. 1; +, transcripts detected, but representing less than 0.2% of the total *NOS1* mRNA. Right: Analyses of promoter activities of the 5′ flanking regions of the different first exons of human *NOS1* (exons 1a to 1l). The human cell lines A673, SK-N-MC, and HaCaT, as well as the murine myoblast cell line C2C12, transiently transfected with one of the various *NOS1* gene promoter constructs and a *Renilla* luciferase coreporter, were assayed 24 h later. Data represent means ± SEM of at least three experiments performed in duplicate. Normalized *Photinus* luciferase activities are given as fold of the promoterless vector control pGL3-Basic (B), indicated by the white bar and the horizontal line. Activities of the larger promoter fragments are indicated by black bars, those of the derived 5′–3′-deletion constructs by gray bars (see Fig. 2B for details).

the full-length construct (2.5-fold over pGL3-Basic). The expression of exon 1k in SK-N-MC cells (Fig. 3, left) was paralleled by reporter activity of the respective full-length construct 5-fold over pGL3-Basic. In contrast, the truncated construct had no promoter activity. The low or absent expression of all other exon 1 species in SK-N-MC cells corresponded to the low or absent activity of the respective promoter constructs (Fig. 3, right). As observed in A673 cells, in SK-N-MC cells, the reporter constructs of nonexpressed exon 1a displayed substantial activity (4.5- and 20.5-fold, respectively).

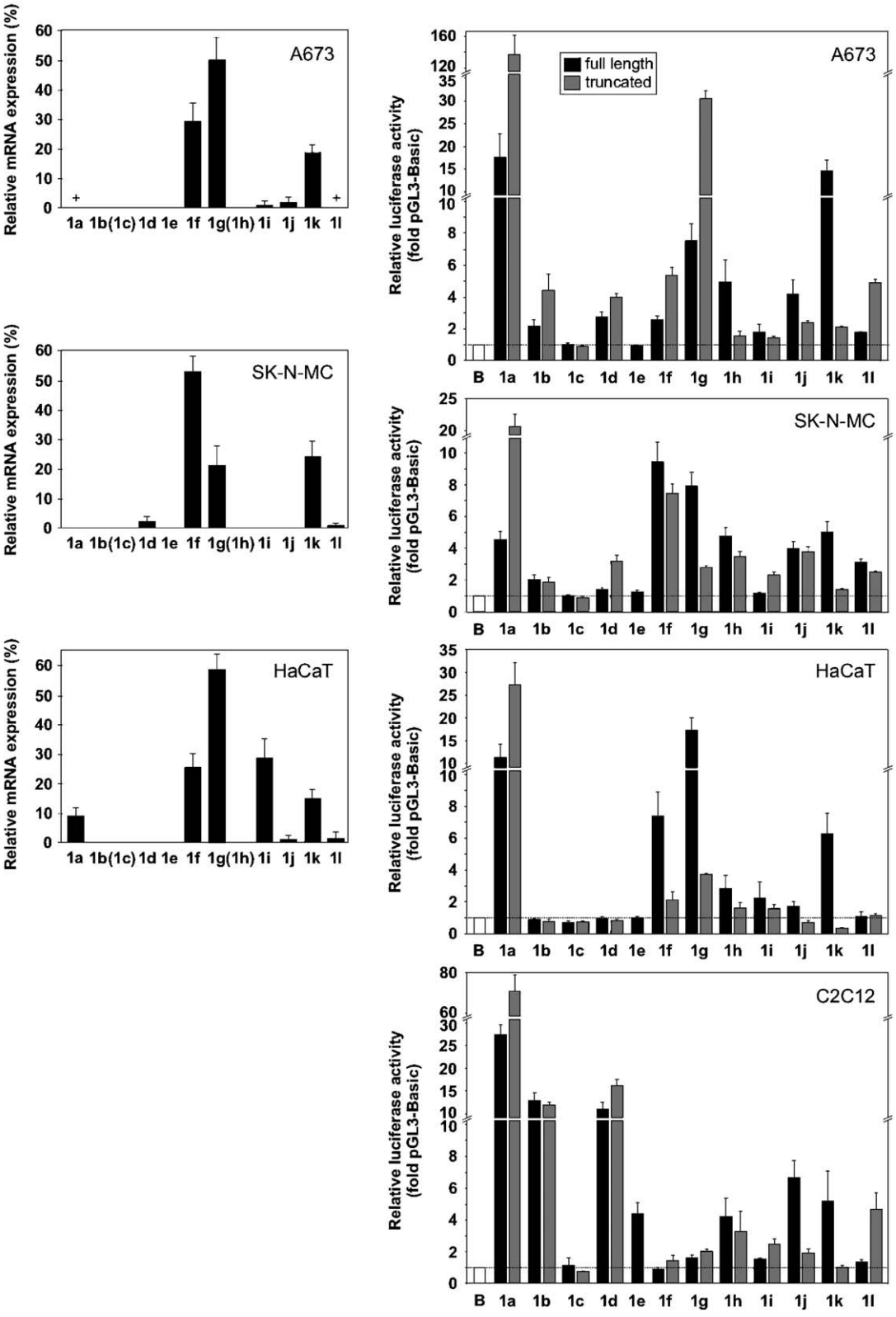

In keratinocyte-like HaCaT cells, the endogenous expression levels of adjacent exons 1f and 1g were reflected by the activities of the respective full-length promoter constructs (7- and 17-fold over pGL3-Basic). Interestingly, both truncated constructs showed a marked decrease in activity (down to 2- and 3.5-fold over pGL3-Basic, respectively). This is suggestive of a cell-type-specific enhancer function due to *cis*-acting regions located upstream of either core promoter. In agreement with the endogenous expression state, the full-length promoter of exon 1k was moderately active (6.2-fold over pGL3-Basic), while the respective deletion construct lacked promoter activity. In contrast to its substantial expression level, the exon 1i-associated full-length promoter construct showed only 2.3-fold the activity of pGL3-Basic, and the corresponding core promoter had very little activity. In accordance with the low or absent expression of exons 1b, 1c, 1d, 1e, 1j, and 1l in HaCaT cells (Fig. 3, left), the corresponding reporter construct showed very little or no activity (Fig. 3, right). As observed in the brain-derived cell lines, the reporter constructs of exon 1a showed high activity (12- and 27-fold over pGL3-Basic, respectively; Fig. 3, right), although exon 1a is only a minor transcript in HaCaT cells (Fig. 3, left).

In human skeletal muscle (and also in heart), there was a marked expression of exon 1d (Fig. 1). Accordingly, in C2C12

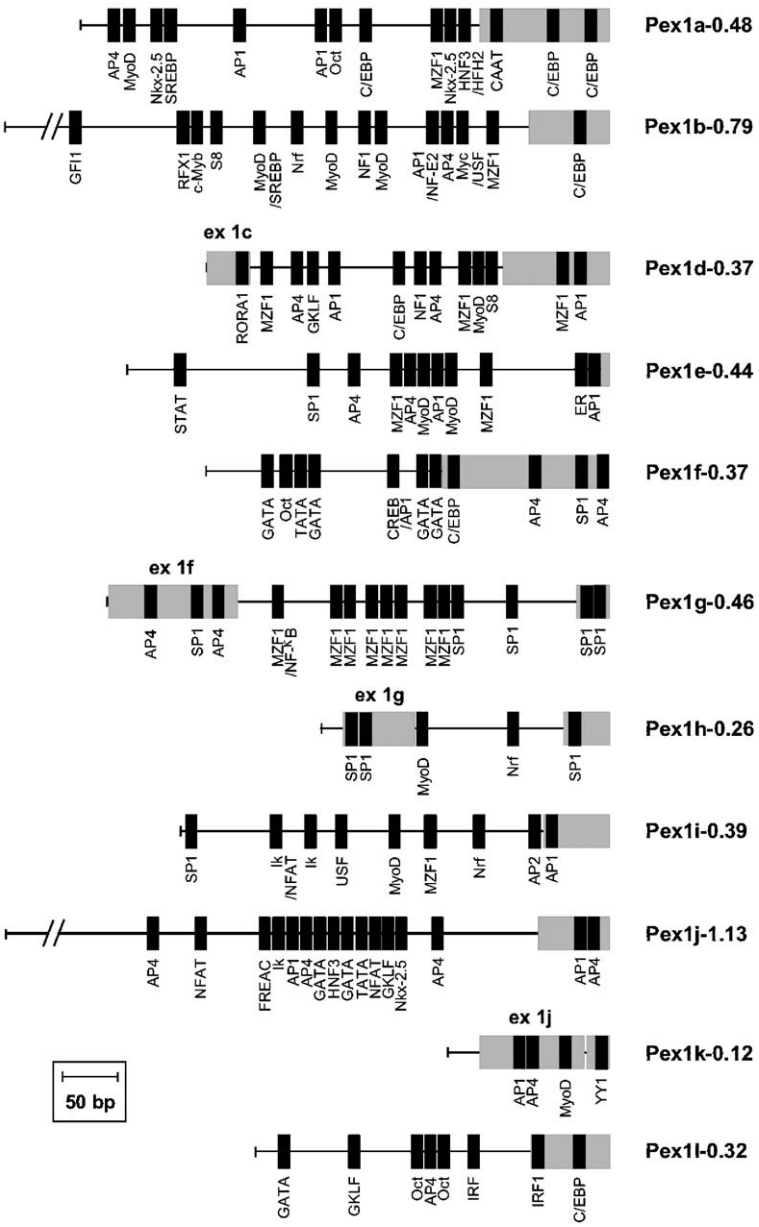

Fig. 4. Scheme of potential transcription factor binding sites within the 5′–3′ truncated constructs of the various *NOS1* promoters. Included exonic sequences are indicated by gray boxes. If the construct contained an additional exon located upstream it is indicated accordingly. Potential transcription factor binding sites were identified by MatInspector v2.2 [34] and are indicated by black boxes and labeled. For the longer promoter reporter constructs, only potential binding sites within the proximal 500 bp have been indicated.

cells, the reporter constructs corresponding to exon 1d displayed 11- and 16-fold activity over pGL3-Basic, respectively (Fig. 3, right). Surprisingly, however, reporter constructs corresponding to exons 1a and 1b were equally active or even more active (Fig. 3, right) although these exons were expressed at only very low levels in skeletal muscle (Fig. 1). Promoter constructs corresponding to other exons (1h, 1j, and 1k) showed some activity (Fig. 3, right), although these exons were expressed at only very low levels in tibialis muscle.

In all three cell types (A673, SK-NM-C, and HaCaT cells) the more active *NOS1* promoters were stronger than the moderately active SV40 promoter. The vector pGL3-Promoter (containing the SV40 promoter) showed 8.24 ± 0.65-fold the activity of pGL3-Basic in A673 cells, 3.24 ± 0.2-fold the activity of pGL3-Basic in SK-N-MC cells, 4.48 ± 0.31-fold the activity of pGL3-Basic in HaCaT cells, and 56.64 ± 10.04-fold the activity of pGL3-Basic in C2C12 cells. However, none of the *NOS1* promoters reached the strength of the vector pGL3-Control (containing the SV40 promoter/enhancer). pGL3-Control showed 163.84 ± 11.25-fold the activity of pGL3-Basic in A673 cells, 55.56 ± 7.73-fold the activity of pGL3-Basic in SK-N-MC cells, 58.25 ± 12.91-fold the activity of pGL3-Basic in HaCaT cells, and 132.18 ± 22.04-fold the activity of pGL3-Basic in C2C12 cells.

Cell-type-specific stimulation of exon 1f and exon 1g promoter activities

We have recently demonstrated in neuronal- and keratinocyte-like cells [6] that human *NOS1* expression is increased upon stimulation with various cAMP-activating agents. This is due to increased transcriptional usage of exon 1f and/or 1g. Interestingly, in the rat, stimulation of *NOS1* expression in pituitary gonadotrope cells was found to rely on a CRE site located closely upstream of exon 1p homologous to exon 1f in human *NOS1* [10]. Since computational analyses (Fig. 4) showed a conservation of this CRE site in humans, we tested its functional relevance in human cells. We assessed the relative activities of test constructs containing the exon 1f/1g promoter region upon treatment with the protein kinase A-activating compound dibutyryl-cAMP (db-cAMP). In SK-N-MC cells, both the exon 1f full-length and the corresponding truncated reporter construct (which still harbors the putative CRE site, Figs. 4 and 5) showed an increase in reporter activity upon stimulation. The same extent of stimulation was obtained with the full-length exon 1g-related promoter containing the CRE site (Fig. 5). However, the respective 5′–3′-deletion construct lacking the CRE site (Figs. 4 and 5) showed decreased basal activity and was not stimulated by db-cAMP.

These findings indicate a functional role for the conserved CRE site located upstream of exon 1f in mediating inducibility of *NOS1* expression by db-cAMP.

Taken together, we have demonstrated that expression of 11 of the 12 described exon 1 variants of the human *NOS1* gene is facilitated by exon-specific promoters. Moreover, the overall pattern of cell-type-specific promoter activities was in broad agreement with the expression profile of the endogenous exon 1 species in the respective cells.

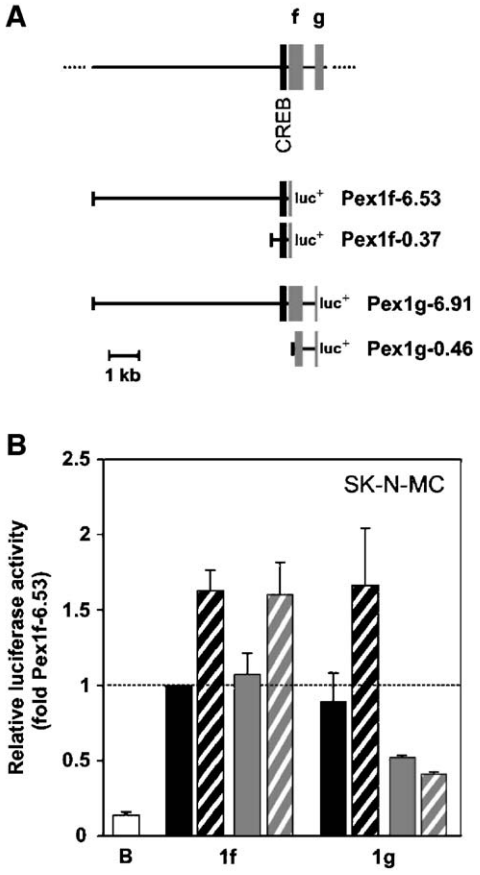

Fig. 5. (A) Scheme of the genomic region of the *NOS1* gene harboring exons 1f and 1g (top). Shown below are reporter constructs containing the 5′ flanking regions of exons 1f and 1g of human *NOS1* and 5′–3′-deletion constructs thereof. A conserved CRE binding site of potential functional importance (see B) is indicated. (B) Effect of dibutyryl-cAMP on the activity of the human *NOS1* promoter related to exons 1f and 1g. Activities of the full-length (black columns) and truncated (gray columns) promoter reporter constructs associated with exons 1f and 1g were assessed in the neuroblastoma cell line SK-N-MC. Activities were determined under basal conditions (solid columns) and following stimulation with dibutyryl-cAMP (300 μM for 12 h, hatched columns). Normalized *Photinus* luciferase activities are given as fold of basal activity of the parental exon 1f promoter reporter construct (Pex1f-6.53). The promoterless pGL3-Basic (B) was included as a negative control. Values represent means ± SEM of three or more experiments performed in duplicate.

Discussion

In this study, we have analyzed the cell-type-specific expression pattern of the multiple exon 1 variants of the human *NOS1* gene. For 11 of the 12 described *NOS1* exon 1 variants we have demonstrated that expression was facilitated by individual exon-flanking promoters. Our data confirm previous results, which demonstrated cell-type-specific usage of a total of 12 different *NOS1* exon 1 variants [6,11] and the predominant expression of exons 1d, 1f, and 1g in various cell types [6]. To our knowledge, the human *NOS1* gene displays the highest number of alternative promoters described so far. In many cases, the activity of the exon 1-specific promoters

corresponded to the endogenous expression level of the respective exon 1 variant.

The multiple exon 1 sequences of the human *NOS1* gene (1a–1l) are scattered over approximately 50 kb of genomic region [6] with exons 1b to 1d and exons 1f to 1k clustered within a short range. Notably, in mouse and rat, only three [12] and six [10,13] alternative *NOS1* exon 1 variants, respectively, have been characterized so far. Exons 1f and 1g are the only variants conserved between human and rodents (in mouse designated exons 1a and 1b, in rat exons 1a and 1p). Whereas in humans, both exons are separated by about 300 bp, they are merged in rodents [10,12,14]. Exons 1f and 1g were also the first *NOS1* exon 1 variants described in humans, and the corresponding 5′ flanking genomic regions were previously shown to exert promoter activity [14]. While the promoter of exon 1f could be stimulated by nerve growth factor [15], activity of a promoter construct encompassing also the core promoter region of exon 1g was enhanced by phorbol myristate acetate [16]. In humans, other than the dual promoter region of exons 1f and 1g, only the promoter of exon 1d, which is highly expressed in brain, skin, heart, and skeletal muscle (Fig. 1), has been analyzed in detail [17]. In patients with infantile hypertrophic pyloric stenosis, *NOS1* expression is strongly decreased in pyloric tissue due to downregulated transcriptional activity of exon 1d, which is the result of distinct promoter polymorphisms in some cases [18]. In these patients, a compensatory upregulation of exon 1f transcription was noted.

We have previously shown that stimulation of CREB activity results in increased *NOS1* expression as a consequence of enhanced transcription of exons 1f/1g [6]. This is likely to be mediated by a CRE binding site located immediately upstream of exon 1f (see Fig. 5). Among the numerous stimuli known to affect *NOS1* expression, steroid hormones were found to upregulate *NOS1* in several cell types [19], while corticosteroids decreased *NOS1* expression [20]. In response to lipopolysaccharide, which induces expression of proinflammatory cytokines, and upon direct application of IFN-γ, *NOS1* expression was either up- or downregulated in a cell-type-specific manner [19,21]. However, the molecular basis for the regulation of the *NOS1* gene by these agents has been scarcely analyzed and may involve both transcriptional and posttranscriptional mechanisms. For example, we have recently demonstrated that *NOS1* expression in keratinocytes was increased upon stimulation with epidermal growth factor (EGF) and contributed to keratinocyte proliferation. EGF enhanced the level of exon 1i + 1k *NOS1* mRNA due to increased mRNA stability [6,8]. Moreover, Wang et al. [5] have demonstrated that the different *NOS1* exon 1 variants exert cell-type-dependent differential translational efficiency. Inclusion of exon 1k into *NOS1* mRNA reduced in most cases the rate of translation, forming a stem–loop structure, which interacts with an RNA binding protein complex [22].

Taken together, the human *NOS1* gene is highly complex in terms of expressional regulation given the high number of 11 identified promoter regions and posttranscriptional mechanisms affecting mRNA stability and/or translational efficacy of the various noncoding *NOS1* exon 1 variants. All of these mechanisms may interact to ensure a fine-tuned expressional control of *NOS1* in various cell types under normal and stimulated conditions. Although most genes are controlled in expression by a single promoter and harbor only one exon 1, a survey of the human genome has revealed around 3000 genes with more than one exon 1. Most of these genes (79%) contain two different exon 1 variants [23]. Among them are the human growth hormone receptor gene comprising a total of nine different untranslated exon 1 variants [24] and the human nuclear respiratory factor 1 gene, which exhibits at least six different noncoding alternative exon 1 variants characterized by differential translational efficiency [25].

Dysregulated *NOS1* expression has been implicated in the pathogenesis of neurodegenerative disorders such as stroke [26], Parkinson disease [27], Alzheimer disease [28], and amyotrophic lateral sclerosis [29]. Excessive formation of NO and its metabolite peroxynitrite may be neurotoxic [30]. But under distinct conditions of cellular stress, NO was shown to exert neuroprotective effects [31]. In neuronal cells, *NOS1* expression is enhanced under conditions of cellular stress and injury and is linked to the activity of neurotransmitters [7,19]. Given the important role of *NOS1* in both physiologic and pathophysiologic conditions, our findings allow us to elucidate which exon 1-flanking promoters are involved in *NOS1* regulation in a given cell type and which pharmacological agents may affect distinct *NOS1* promoters to influence overall *NOS1* expression clinically.

Materials and methods

Human tissues

Human biopsies were obtained from the hospitals of the Johannes Gutenberg University, Mainz, Germany, and the Albert Ludwig University, Freiburg, Germany, according to the guidelines of the Human Ethical Committees of the two universities. Tissue samples were either processed immediately or frozen in dry ice and stored at −70°C.

Cell lines

The human neuroepithelial cell line A673, the human neuroblastoma cell line SK-N-MC, the human keratinocyte cell line HaCaT [32], and the murine myoblast cell line C2C12 were grown in Dulbecco's modified Eagle's medium (DMEM; Invitrogen, Groningen, The Netherlands) supplemented with 10% of fetal calf serum, 2 mM L-glutamine, and 100 U/ml penicillin/streptomycin (PAA, Pasching, Austria). Cells were maintained in a 10% CO_2 incubator at 37°C.

Quantification of the various first exon NOS1 mRNAs by RT real-time PCR

Quantification of the distinct first exon *NOS1* messages was obtained by two-step RT real-time PCR using the iCyler (Bio-Rad, Munich, Germany). Total RNA (10 to 25 μg), isolated from human biopsies or cell lines, was reverse transcribed with the Omniscript RT kit (Invitrogen). An *NOS1*-specific antisense primer was used to prime the reverse transcription (*NOS1* RT, exons 5 and 6, 5′-GGAGCCAAATCTTTTAATTGATGA-3′; GenBank, NM_000620: 1822–1799). PCR were performed on 1/25 aliquots of the RT reaction with the QuantiTect Probe PCR kit (Qiagen, Hilden, Germany) as recommended by the manufacturer. For the detection of the various *NOS1* transcripts, oligonucleotides specific for each first exon were used as sense primers (Table 1); an exon 2

Table 1
Specific first exon sense primers used for RT real-time PCR

Name	Sequence
*NOS1*a S	5′-CCCCTCCCTTGAGGAGCT-3′
*NOS1*b S	5′-CCCATGCTCTAGCTTGGAGC-3′
*NOS1*d S	5′-ATGCCAGGGTGAGGCCTT-3′
*NOS1*e S	5′-CTAAGAAGAAGGAGGAGGAGGAA-3′
*NOS1*f S	5′-CCGAGCGGACGGGCTC-3′
*NOS1*g S	5′-TGCCCGGCTCGGCGT-3′
*NOS1*g2 S	5′-CGGCTCGGCGTCAGCTC-3′
*NOS1*gk S	5′-GGCTCGGCGTCAGGTTG-3′
*NOS1*i S	5′-CCCCTGGGTTCTGGTCCTA-3′
*NOS1*i2 S	5′-TGTTGCGTGACCTTCGCT-3′
*NOS1*ik S	5′-TTGCGTGACCTTCGGTTG-3′
*NOS1*jk S	5′-GGAGCCTCTTAACTTTCAGGTTG-3′
*NOS1*k S	5′-AGCCATAGTCACCTAGCTGCTC-3′
*NOS1*L2 S	5′-AGACTTCAAGATGATCGTGCAAA-3′

sequence, 5′-CGTCTGATGGCTGTGTCTAGAAGT-3′, was used as antisense primer; and 5′-6FAM-TTCATTGCCAGCCTGTTAGATGCGGAT-TAMRA was used as the fluorescent TaqMan probe. PCR conditions were initial activation of the polymerase at 95°C for 15 min and 45 cycles of denaturation at 95°C for 15 s and annealing/extension at 60°C for 1 min. Fluorescence was monitored at each cycle during the annealing/extension step.

Isolation and subcloning of the human NOS1 promoter regions

We obtained two PAC clones from the Ressourcenzentrum/Primärdatenbank of the German Human Genome Project at the Max-Planck Institute for Molecular Genetics (Berlin, Germany), which encompass adjacent genomic regions of the *NOS1* gene locus on chromosome 12q24.2–q24.3. They respectively harbor exons 1a–1e (RP11-227B21) and exons 1f–1l (RP11-33101) and the respective 5′ flanking genomic regions. For both PAC clones, the genomic sequence had been determined (GenBank Accession Nos. AC073864 and AC068799).

As outlined in Fig. 2A, the multiple *NOS1* exon 1 variants are located within about 45 kb of the genomic sequence. Notably, both skeletal muscle-specific exons 1b–1d and neuronal-specific exons 1f–1k form two clusters, with single exons separated by a few hundred base pairs in many cases [6].

PAC clone DNA was digested with restriction enzymes *Pst*I, *Sma*I (RP11-227B21), and *Acc*65I (RP11-227B21, RP11-33101) in parallel reactions. Restriction fragments were cloned into appropriately linearized pZero-2.1 (Invitrogen). Transformants were used to generate colony filters in duplicate. To generate exon 1-specific hybridization probes, 5′-RACE clones that harbored exons 1a, 1d, 1e, 1f, and 1l were used as templates for PCR. Exon sequences were amplified by using an appropriate exon 1 sense and exon 2 antisense primer [6]. PCR products were labeled by incorporation of digoxigenin-11–dUTP (Roche Diagnostics, Mannheim, Germany). Probe-specific colonies were identified by colony filter hybridization as recommended by the manufacturer.

Construction of promoter reporter constructs

To generate promoter construct Pex1a-7.1, an isolated 9.4-kb *Pst*I fragment was digested with *Apa*LI, which cuts at +116 bp relative to the transcription start point, and 5′ overhangs were filled in using the Klenow enzyme. A 7.1-kb promoter fragment was excised by a sequential digest with *Acc*65I that cuts adjacent to the 5′-fragment end within the pZero2.1 polylinker. Promoterless *Photinus* luciferase reporter vector pGL3-Basic (Promega, Heidelberg, Germany) was double-digested with *Acc*65I and *Sma*I and ligated with the exon 1a promoter fragment. To obtain a promoter construct for exon 1b, an isolated 5.9-kb *Sma*I fragment was digested with *Ecl*136II, which excised a 785-bp fragment, including 72 bp of exon 1b and 5′ flanking sequence. This *Ecl*136II fragment was cloned into *Sma*I-linearized pGL3-Basic, thereby obtaining Pex1b-0.79. Afterward, the 5.9-kb *Sma*I fragment was double-digested with *Acc*65I (see above) and *Sca*I, which cuts 539 bp upstream of exon 1b. To obtain Pex1b-5.03, this fragment was ligated with Pex1b-0.79 digested likewise. An isolated 2.9-kb *Acc*65I PAC restriction fragment, encompassing exons 1c and 1d, was double-digested with *Acc*65I and *Stu*I, which cuts within exon 1d at +96 bp, and cloned into *Acc*65I/*Sma*I double-digested pGL3-Basic (Pex1d-2.0). This construct was double-digested with *Bst*API, which cuts within exon 1c, and *Bgl*II, which cuts within the downstream pGL3-Basic polylinker. Restriction site overhangs were polished by treatment with mung bean nuclease and religated, thereby generating Pex1c-1.65, which included 29 bp of exon 1c. Reporter constructs Pex1c-1.65, Pex1d-2.0, and the 5.9-kb *Sma*I fragment were digested with *Acc*65I (see above). The excised exon 1c/1d 5′ flanking region derived from the *Sma*I PAC subclone was ligated with both of the precut luciferase reporter constructs, thereby generating Pex1c-6.9 and Pex1d-7.27. Due to great difficulties in cloning a PAC clone restriction fragment spanning exon 1e, we switched to a PCR-based approach. By using PAC clone RP11-227B21 as template, proofreading *Pwo* DNA polymerase, and primers 1e-sense (5′-TGTATTTCAAAATAGCTAGAAGAGAGGAAT-3′) and 1e-antisense (5′-CACAATGGGCATTTGCCTAACAAAATA-3′), we amplified a 2.57-kb fragment that spans 2 kb of the exon 1e 5′ flanking region and exon 1e. However, we were not successful in cloning this PCR product. We subcloned a 439-bp fragment, obtained by *Nhe*I/*Bam*HI double-digest of the 2.57-kb PCR product, that includes 8 bp of exon 1e (Pex1e-0.44). An isolated 9-kb *Acc*65I fragment harboring exons 1f–1k was digested with *Eag*I (+126 bp of exon 1f), *Acc*I (+42 bp of exon 1h), *Bsa*I (+64 bp of exon 1j), and *Eco*RI (+19 bp of exon 1k), and 5′ overhangs were filled in by treatment with Klenow enzyme. The respective promoter fragments were excised by *Acc*65I digestion and were subcloned into pGL3-Basic, double-digested with *Acc*65I and *Sma*I. Thereby, we generated Pex1f-6.53, Pex1h-7.13, Pex1j-8.97, and Pex1k-9.02. To obtain a promoter construct for exon 1g, the 9-kb *Acc*65I fragment was digested with *Fsp*I, and a resulting 1.47-kb fragment, cutting at +21 within exon 1g, was subcloned into *Sma*I-linearized pGL3-Basic. This construct and the 9-kb *Acc*65I fragment were double-digested with *Acc*65I and *Nde*I, which cuts 1.2 kb upstream of exon 1g. The excised region was ligated with the proximal putative promoter region of exon 1g, thereby generating Pex1g-6.91. Pex1i-7.88 was obtained by digesting the 9-kb *Acc*65I fragment with *Acc*65I and *Xba*I, as the latter cuts at +59 bp within exon 1i, and the excised promoter fragment was ligated with *Acc*65I/*Nhe*I double-digested pGL3-Basic. To obtain a promoter construct for exon 1l, an isolated 15.8-kb *Acc*65I fragment was used as template for PCR. By employing proofreading *Pwo* DNA polymerase, vector-specific M13 reverse primer (5′-CAGGAAACAGCTATGAC-3′), and an exon 1l-specific antisense primer (5′-TCTACTGAGAGTGACGCAGCA-3′), a 1.83-kb PCR product was generated that included 71 bp of exon 1l. This PCR product was digested with *Acc*65I and cloned into *Acc*65I/*Sma*I double-digested pGL3-Basic. The sizes and locations of the generated *NOS1* promoter constructs are depicted in Fig. 2B.

We also generated a series of 5′–3′-deletion constructs for the different exon 1 variants, which are depicted in Fig. 2B. The reporter constructs Pex1b-0.79 and Pex1c-1.65 had been obtained as by-products in the course of generating the set of *NOS1* promoter constructs (see above). To generate the other deletion promoter constructs, the respective parental promoter construct was double digested with *Acc*65I, which cuts at the 5′ end in all cases. The linearized reporter constructs were digested in addition with *Afl*II (Pex1a-7.1), *Sma*I (Pex1h-7.13), *Spe*I (Pex1k-9.02), *Bst*API (Pex1d-7.27), *Sac*II (Pex1i-7.88), and *Ecl*136II (Pex1l-1.83). In the case of protruding 5′ overhangs, double-digested reporter constructs were end-polished by treatment with Klenow enzyme and religated, thereby generating Pex1h-0.26 and Pex1k-0.12. In the case of 3′ overhangs, respective reporter constructs were treated with mung bean nuclease and religated, thereby obtaining Pex1d-0.37 and Pex1i-0.39. The parental promoter constructs for exon 1f (*Nco*I), exon 1g (*Ecl*136II), and exon 1j (*Ecl*136II) were digested with the restriction enzyme indicated. The excised fragments that harbor the respective proximal promoter region were ligated with likewise linearized pGL3-Basic, thereby generating Pex1f-0.37, Pex1g-0.46, and Pex1j-1.13.

Transient transfection and luciferase assays

For transient transfection, cells were seeded in wells of a 24-well cluster plate at a density of 5×10^5 cells per well. Cells were transfected on the following day with 950 ng of the largest promoter test construct and equimolar

amounts of shorter test constructs. To correct for differences in transfection efficiency, cells were cotransfected with 50 ng of a *Renilla* luciferase expression vector driven by the human elongation factor 1α1 gene promoter [33]. In experiments conducted to test for the stimulatory activity of dibutyryl-cAMP (Sigma, Deisenhofen, Germany), pRL-SV40 (Promega) served as an internal control for transfection efficiency. Degraded salmon sperm DNA (Roche Diagnostics) was added as necessary to obtain a total of 1 μg of DNA. The DNA mixture was incubated with 1.5 μl (A673, SK-N-MC) or 1 μl (HaCaT, C2C12) of liposomal transfection reagent Fugene 6 (Roche Diagnostics). Test constructs were tested in duplicate in at least three independent experiments. Luciferase activities were measured 24 h after transfection. Relative promoter activities were determined as the ratio of *Photinus* and *Renilla* luciferase activity.

Acknowledgments

We thank Thomas J. Feuerstein (Department of Neurology, Section for Clinical Neuropharmacology, Albert Ludwigs University, Freiburg, Germany) for the supply of human brain tissue. We are indebted to the following individuals from the Johannes Gutenberg University Hospitals, Mainz, Germany, for the various human biopsy and autopsy specimens: Theo Junginger (Abdominal Surgery), Pol M. Rommens and Martin Hessmann (Traumatology), Joachim W. Thüroff (Urology), Reinhard Urban (Forensic Medicine), and Jürgen Knop (Dermatology). We also thank Dr. Norbert E. Fusenig, German Cancer Research Center (DKFZ, Heidelberg, Germany), for providing the HaCaT cell line. This study was supported by Collaborative Research Center SFB 553 (Project A6 to U.F.) from the Deutsche Forschungsgemeinschaft, Bonn, Germany.

References

[1] K.S. Christopherson, D.S. Bredt, Nitric oxide in excitable tissues: physiological roles and disease, J. Clin. Invest. 100 (1997) 2424–2429.
[2] H. Prast, A. Philippu, Nitric oxide as modulator of neuronal function, Prog. Neurobiol. 64 (2001) 51–68.
[3] M. Colasanti, H. Suzuki, The dual personality of NO, Trends Pharmacol. Sci. 21 (2000) 249–252.
[4] U. Förstermann, J.P. Boissel, H. Kleinert, Expressional control of the 'constitutive' isoforms of nitric oxide synthase (NOS I and NOS III), FASEB J. 12 (1998) 773–790.
[5] Y. Wang, et al., RNA diversity has profound effects on the translation of neuronal nitric oxide synthase, Proc. Natl. Acad. Sci. USA 96 (1999) 12150–12155.
[6] J.P. Boissel, M. Zelenka, U. Gödtel-Armbrust, T.J. Feuerstein, U. Förstermann, Transcription of different exons 1 of the human neuronal nitric oxide synthase gene is dynamically regulated in a cell- and stimulus-specific manner, Biol. Chem. 384 (2003) 351–362.
[7] J.P. Boissel, M. Bros, A. Schröck, U. Gödtel-Armbrust, U. Förstermann, Cyclic AMP-mediated upregulation of the expression of neuronal NO synthase in human A673 neuroepithelioma cells results in a decrease in the level of bioactive NO production: analysis of the signaling mechanisms that are involved, Biochemistry 43 (2004) 7197–7206.
[8] J.P. Boissel, et al., The neuronal nitric oxide synthase is upregulated in mouse skin repair and in response to epidermal growth factor in human HaCaT keratinocytes, J. Invest. Dermatol. 123 (2004) 132–139.
[9] D. Blottner, G. Luck, Nitric oxide synthase (NOS) in mouse skeletal muscle development and differentiated myoblasts, Cell Tissue Res. 292 (1998) 293–302.
[10] L.K. Bachir, J.N. Laverriere, R. Counis, Isolation and characterization of a rat nitric oxide synthase type I gene promoter that confers expression and regulation in pituitary gonadotrope cells, Endocrinology 142 (2001) 4631–4642.
[11] Y. Wang, D.C. Newton, P.A. Marsden, Neuronal NOS: gene structure, mRNA diversity, and functional relevance, Crit. Rev. Neurobiol. 13 (1999) 21–43.
[12] M. Sasaki, et al., Dynamic regulation of neuronal NO synthase transcription by calcium influx through a CREB family transcription factor-dependent mechanism, Proc. Natl. Acad. Sci. USA 97 (2000) 8617–8622.
[13] I. Oberbaumer, D. Moser, S. Bachmann, Nitric oxide synthase 1 mRNA: tissue-specific variants from rat with alternative first exons, Biol. Chem. 379 (1998) 913–919.
[14] J. Xie, P. Roddy, T.K. Rife, F. Murad, A.P. Young, Two closely linked but separable promoters for human neuronal nitric oxide synthase gene transcription, Proc. Natl. Acad. Sci. USA 92 (1995) 1242–1246.
[15] T.K. Rife, J. Xie, C. Redman, A.P. Young, The 5′2 promoter of the neuronal nitric oxide synthase dual promoter complex mediates inducibility by nerve growth factor, Brain Res. Mol. Brain Res. 75 (2000) 225–236.
[16] A.P. Young, F. Murad, H. Vaessin, J. Xie, T.K. Rife, Transcription of the human neuronal nitric oxide synthase gene in the central nervous system is mediated by multiple promoters, Adv. Pharmacol. 34 (1995) 91–112.
[17] D. Saur, B. Seidler, H. Paehge, V. Schusdziarra, H.D. Allescher, Complex regulation of human neuronal nitric-oxide synthase exon 1c gene transcription: essential role of Sp and ZNF family members of transcription factors, J. Biol. Chem. 277 (2002) 25798–25814.
[18] D. Saur, et al., Single-nucleotide promoter polymorphism alters transcription of neuronal nitric oxide synthase exon 1c in infantile hypertrophic pyloric stenosis, Proc. Natl. Acad. Sci. USA 101 (2004) 1662–1667.
[19] J.P. Boissel, P.M. Schwarz, U. Förstermann, Neuronal-type NO synthase: transcript diversity and expressional regulation, Nitric Oxide Biol. Chem. 2 (1998) 337–349.
[20] P.M. Schwarz, B. Gierten, J.P. Boissel, U. Förstermann, Expressional down-regulation of neuronal-type nitric oxide synthase I by glucocorticoids in N1E-115 neuroblastoma cells, Mol. Pharmacol. 54 (1998) 258–263.
[21] I. Gath, U. Gödtel-Armbrust, U. Förstermann, Expressional down-regulation of neuronal-type NO synthase I in guinea pig skeletal muscle in response to bacterial lipopolysaccharide, FEBS Lett. 410 (1997) 319–323.
[22] D.C. Newton, et al., Translational regulation of human neuronal nitric-oxide synthase by an alternatively spliced 5′-untranslated region leader exon, J. Biol. Chem. 278 (2003) 636–644.
[23] T. Zhang, P. Haws, Q. Wu, Multiple variable first exons: a mechanism for cell- and tissue-specific gene regulation, Genome Res. 14 (2004) 79–89.
[24] C.G. Goodyer, et al., Organization and evolution of the human growth hormone receptor gene 5′-flanking region, Endocrinology 142 (2001) 1923–1934.
[25] L. Huo, R.C. Scarpulla, Multiple 5′-untranslated exons in the nuclear respiratory factor 1 gene span 47 kb and contribute to transcript heterogeneity and translational efficiency, Gene 233 (1999) 213–224.
[26] S. Love, Oxidative stress in brain ischemia, Brain Pathol. 9 (1999) 119–131.
[27] S. Hunot, et al., Nitric oxide synthase and neuronal vulnerability in Parkinson's disease, Neuroscience 72 (1996) 355–363.
[28] P.J. Norris, R.L. Faull, P.C. Emson, Neuronal nitric oxide synthase (*NOS1*) mRNA expression and NADPH-diaphorase staining in the frontal cortex, visual cortex and hippocampus of control and Alzheimer's disease brains, Brain Res. Mol. Brain Res. 41 (1996) 36–49.
[29] M.V. Catania, E. Aronica, B. Yankaya, D. Troost, Increased expression of neuronal nitric oxide synthase spliced variants in reactive astrocytes of amyotrophic lateral sclerosis human spinal cord, J. Neurosci. 21 (2001) RC148.
[30] M. Lafon-Cazal, S. Pietri, M. Culcasi, J. Bockaert, NMDA-dependent superoxide production and neurotoxicity, Nature 364 (1993) 535–537.

[31] T. Andoh, S.Y. Lee, C.C. Chiueh, Preconditioning regulation of bcl-2 and p66shc by human NOS1 enhances tolerance to oxidative stress, FASEB J. 14 (2000) 2144–2146.
[32] P. Boukamp, et al., Normal keratinization in a spontaneously immortalized aneuploid human keratinocyte cell line, J. Cell Biol. 106 (1988) 761–771.
[33] D.W. Kim, T. Uetsuki, Y. Kaziro, N. Yamaguchi, S. Sugano, Use of the human elongation factor 1 alpha promoter as a versatile and efficient expression system, Gene 91 (1990) 217–223.
[34] K. Quandt, K. Frech, H. Karas, E. Wingender, T. Werner, MatInd and MatInspector: new fast and versatile tools for detection of consensus matches in nucleotide sequence data, Nucleic Acids Res. 23 (1995) 4878–4884.